# Structure and Rheology of Mixed Polymeric Micelles Formed by Hydrophobically End-Capped Poly(ethylene oxide)

**ARTICLE** *in* MACROMOLECULES · AUGUST 2008

Impact Factor: 5.8 · DOI: 10.1021/ma800556u



**3 AUTHORS:**

Frédéric Renou
Université du Havre
**14** PUBLICATIONS **135** CITATIONS
SEE PROFILE

Lazhar Benyahia
Université du Maine
**69** PUBLICATIONS **703** CITATIONS
SEE PROFILE

Taco Nicolai
Université du Maine
**219** PUBLICATIONS **5,230** CITATIONS
SEE PROFILE

# Structure and Rheology of Mixed Polymeric Micelles Formed by Hydrophobically End-Capped Poly(ethylene oxide)

**Frédéric Renou, Lazhar Benyahia, and Taco Nicolai***

*Polymères, colloïdes, Interfaces, UMR CNRS 6120, Université du Maine, 72085 Le Mans Cedex 9, France*

**Otto Glatter**

*Institute of Chemistry, University of Graz, Heinrichstrasse 28, A-8010 Graz, Austria*

*Received March 12, 2008; Revised Manuscript Received June 18, 2008*

ABSTRACT: The structure and the rheology of polymeric micelles in aqueous solution were studied using dynamic and static light scattering, small-angle X-ray scattering, and oscillatory shear rheology. The polymeric micelles were formed by association of poly(ethylene oxide) end-capped with octadecyl. These systems show a discontinuous liquid−solid transition at high concentrations and low temperatures. In the solid state domains appear where the micelles have a crystalline order. Two different molar masses of PEO were used, and mixtures with various ratios were investigated. It is shown that in all cases mixed micelles are formed, which influences both the liquid−solid transition and crystal structure. Incorporating small chains in micelles formed by large chains or vice versa allows in both cases to the micelles to flow and leads to disappearance of the crystalline order, but through different mechanisms.

## Introduction

Diblock copolymers that consist of a large soluble block and a relatively small insoluble block associate into starlike polymeric micelles[1] with a small dense core and a large solvated corona formed by the insoluble and soluble blocks, respectively. At high concentrations the micelles fill up the whole space and interpenetrate. As a consequence, they jam in the sense that steric hindrance inhibits flow of the close-packed micelles at low stresses. The flow rate decreases with decreasing stress following a steep power law.[2] This state is sometimes termed a (hard) gel, but we prefer to call it a solid since it is caused purely by repulsion and there is no formation of a cross-linked percolating network. Usually a cubic liquid crystalline order is observed in this state.

Polymeric micelles resemble star polymers, but there are intriguing differences. Star polymers also stop flowing at high concentrations if the association number is sufficiently high, but a crystalline order is almost never observed.[3] These systems may therefore be considered glasses. It was recently shown, however, that for polymeric micelles the liquid−solid transition is also a glass transition and that the crystalline order forms only after the solid is formed.[4] This is similar to the case of hard sphere glasses in which crystals can form slowly. Crystallization of jammed polymeric micelles is much faster than in hard spheres glasses because they are soft and can exchange arms. In the liquid state the viscosity of star polymers[3,5] and also of hard spheres[6] increases sharply but continuously with increasing concentration. The viscosity of polymeric micelles increases first in a similar manner but jumps at a critical concentration discontinuously to an immeasurably high value.[4] Thus, while star polymer solutions can be prepared with any viscosity by careful tuning of the concentration or the temperature, stable (dynamic) polymeric micelle solutions can only be prepared over a limited range of viscosities.

The origin of the difference in behavior between star polymers and polymeric micelles is that the latter can exchange arms, which results in an extra degree of freedom to minimize the free energy. The exchange time can be determined by rheology on difunctionalized polymers and is fast (less than a second) for the systems studied here.[7] The well-defined crystalline order observed in micelle solutions over a broad range of concentrations is probably made possible by a continuous change of the number of arms.

The liquid−solid transition can be induced either by increasing the concentration or by increasing the repulsion between the polymers. The latter can be done by varying the solvent quality for instance by changing the temperature in marginal solvents. In fact, the important parameter that determines the liquid−solid transition is the effective excluded volume of the stars or the micelles.

Addition of linear nonfunctionalized polymer destabilizes the solid state.[8−12] The effect increases with increasing molar mass of these polymers, and only a small weight fraction of large polymers is enough to melt the solid. It is clear that the presence of linear polymers decreases the repulsion between the stars probably involving depletion of the linear chains,[13] but the exact mechanism is not yet elucidated. In particular, the spatial distribution and conformation of the linear polymers has not yet been determined.

An alternative method to modify the solid state and thus the mechanical properties of the system is to mix star polymers or polymeric micelles of different sizes. A recent study of mixtures of star polymers showed that adding small stars to a glass of large stars leads to melting.[14,15] This effect was attributed to a decrease of the repulsion between the large stars by depletion of small stars. If the size ratio was large, the small stars remained mobile. However, if the size ratio was closer to unity, the small stars were immobilized and contributed to the elastic modulus of the solid. Therefore, the destabilizing effect did not increase with increasing size of added star as it does for added linear polymers. Instead, there is an optimum ratio for which the destabilizing effect is maximum.

Mixtures of polymeric micelles based on poly(ethylene oxide) (PEO) with m ethylene oxide units end-capped with an alkyl chain containing *n* carbons (E*m*C*n*) in water have been investigated by Yamazaki et al.[16] This is a good model system because the liquid−solid transition can be easily induced by temperature variations, while the association number (*p*) of the micelles is independent of the temperature. The main difference

* Corresponding author. E-mail: Taco.Nicolai@univ-lemans.fr.

10.1021/ma800556u CCC: $40.75 
Published on Web 08/16/2008

with star polymer mixtures is that polymeric micelles can in principle exchange arms to form mixed micelles. This issue is essential for a proper interpretation of the results, and we will show that it can be resolved by a combination of static and dynamic light scattering. For the system studied here we found that mixed micelles were formed. Yamazaki et al. studied mixtures of E8C12 and E25C12 at high concentrations using rheology and small-angle X-ray scattering (SAXS). Pure solutions of E8C12 formed a hexagonal phase while the larger micelles formed a cubic phase. They observed that mixing of pure systems that are solid and ordered can lead to melting of the solid and the crystalline phase.

Here we extend and complement this work by a study of mixtures of larger PEO micelles (E92C18 and E19C18) that both form cubic phases in pure solutions. The dynamic mechanical properties and the structure were investigated over a broad range of concentrations and temperatures. Understanding the behavior of mixed micelles is important because it allows one to tune the rheological properties of polymeric micelles without synthesizing different polymers. It may also help in understanding the behavior of so-called fuzzy star polymers for which the arm length is not mondisperse.[5]

## Experimental Section

**Materials.** PEO end-capped with octadecyl with two different chains lengths: E92C18 (Brij 700, batch 05214MC) and E19C18 (Brij 78, batch 036K0183) were purchased from Aldrich. The molar masses were 4.3 kg/mol for E92C18 and 1.1 kg/mol for E19C18 as determined by mass spectroscopy (MALDI-TOF), which showed that the molar mass distribution was very narrow for both samples (the ratio of the weight-average to the number-average molar mass was less than 1.1). Clear solutions in pure "Millipore" water were obtained after stirring for an hour at 80 °C. The total PEO concentrations ($C$) were calculated using a density of 1.15 kg/L.[17] The small temperature dependence of the density was ignored. E92C18 was soluble up to about 750 g/L and E19C18 up to about 400 g/L.

Mixtures with different weight fractions ($F$) of E19C18 with respect to the total mass of PEO were prepared by mixing aqueous solutions of the pure systems at 80 °C. Transparent homogeneous solutions were obtained in all cases. For light scattering measurements the samples were filtered through 0.2 $\mu$m pore size Anatop filters when it was possible, while more viscous samples were filtered through 0.45 $\mu$m pore size filters. Highly viscous solutions obtained at the highest concentrations could not be filtered but were purified by ultracentrifugation. We verified that filtration or centrifugation did not modify the PEO concentration.

**Rheology.** Rheology measurements were done on a stress-controlled rheometer (AR2000, TA Instruments) using a cone and plate geometry (diameter 6 cm and angle 0.58° or 4 cm and 2°). The temperature was controlled using a Peltier system. Solvent evaporation was avoided by covering the geometry with mineral oil. Oscillatory measurements were done at 1 Hz with an imposed stress of 10 Pa or an imposed deformation of 0.5% to determine the storage ($G'$) and loss modulus ($G''$). In both cases the measurements were in the linear response regime for the solids and the liquids. For the liquids the dynamic viscosity obtained from $G''$ was the same as the viscosity obtained from flow measurements with an imposed stress of 10 Pa.

**Light Scattering.** Light scattering measurements were made using an ALV-5000 multibit, multitau, full digital correlator in combination with a Spectra-Physics laser emitting vertically polarized light at $\lambda = 532$ nm. The temperature was controlled by a thermostat bath to within ±0.1 °C. The relative excess scattering intensity ($I_r$) was determined as the total intensity minus the solvent scattering divided by the scattering of toluene at 20 °C. $I_r$ is related to the osmotic compressibility ($(d\pi/dC)^{-1}$) and the $z$-average structure factor ($S(q)$):[18,19]

$$I_r = KCRT(d\pi/dC)^{-1}S(q) \quad (1)$$

with $R$ the gas constant and $T$ the absolute temperature.

$$K = \frac{4\pi^2 n^2}{\lambda^4 N_a}\left(\frac{dn}{dC}\right)^2\left(\frac{n_s}{n}\right)^2\frac{1}{R_s} \quad (2)$$

where $N_a$ is Avogadro's number, ($dn/dC$) is the refractive index increment, and $R_s$ is the Rayleigh ratio of toluene. $(n_s/n)^2$ corrects for the difference in scattering volume of the solution with refractive index $n$ and toluene with refractive index $n_s$. $S(q)$ describes the dependence of $I_r$ on the scattering wave vector: $q = (4\pi n/\lambda)\sin(\theta/2)$, with $\theta$ the angle of observation. $R_s = 2.79 \times 10^{-5}$ cm$^{-1}$ at $\lambda = 532$ nm and 20 °C. The refractive index increment of PEO is 0.135 cm$^3$/g,[20,21] and we have assumed that the value for functionalized PEO is the same because the functional group is small. $S(q) = 1$ for $C \to 0$ and $q \to 0$, and the weight-average molar mass ($M_w$) can be calculated as $M_w = I_r/KC$.

The normalized electric field autocorrelation function, $g_1(t)$, was calculated from the measured intensity correlation function, using the so-called Siegert relation.[22] Examples of $g_1(t)$ are shown in Figure 1. $g_1(t)$ was analyzed in terms of a relaxation time ($\tau$) distribution using the REPES routine:[23]

$$g_1(t) = \int A(\tau)\exp(-t/\tau)\,d\tau \quad (3)$$

For all systems a fast $q^2$-dependent relaxation mode was observed caused by the relaxation of the concentration fluctuations of the PEO segments. The cooperative diffusion coefficient was calculated from the average relaxation rate as $D_c = \langle\tau^{-1}\rangle/q^2$. For $C \to 0$ and $q \to 0$ the $z$-average hydrodynamic radius ($R_h$) of the micelles can be calculated using the so-called Stokes−Einstein relation: $R_h = kT/(6\pi\eta D_0)$, with $k$ Boltzmann's constant, $T$ the absolute temperature, and $\eta$ the solvent viscosity.

In addition, a slow diffusional mode was observed at higher PEO concentrations. Slow modes are expected for semidilute star-polymer solutions if the scattering by the dense cores of the stars is significant compared to that of the overlapping PEO segments.[24] Unfortunately, aqueous PEO solutions are well-known to contain a very small weight fraction of large aggregates.[25−27] These aggregates are very difficult to remove completely from the viscous solutions formed at higher concentrations. The relative intensity due to fluctuations of the overlapping PEO segment decreased rapidly with increasing concentration, which explains why the relative amplitude of the fast mode decreased. Therefore, it was not possible to study a slow mode caused by self-diffusion of the micelles, which may or may not be significant in polymeric micelles solutions at higher concentrations. In the following we only discuss the fast mode.

The static light scattering results were corrected for the scattering intensity of the slow mode by multiplying the total intensity with

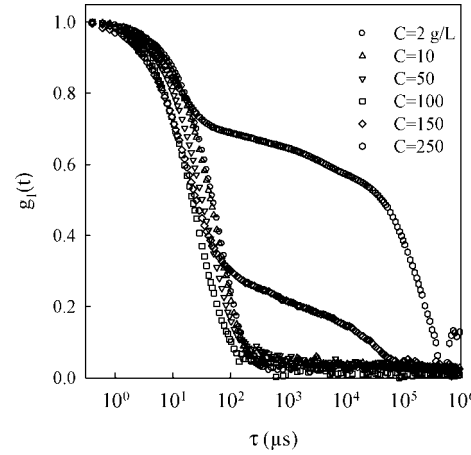


**Figure 1.** Electric field autocorrelation function of mixed micelle solutions ($F = 0.5$) as a function of the PEO concentration.

the relative amplitude of the fast mode. After correction the intensity was found to be independent of $q$ for all samples. The solid samples were nonergodic so that $g_1(t)$ did not fully relax spontaneously. These samples were slowly rotated, which artificially forces $g_1(t)$ to relax with a terminal relaxation time that is determined by the speed of rotation. In this way the correct spatially averaged intensity was recovered.

**SAXS.** Small-angle X-ray scattering (SAXS) measurements were done using a SAXSess camera (Anton Paar, Graz, Austria) connected to an X-ray generator (Philips, PW 3830) operating at 40 kV and 50 mA with a sealed-tube Cu anode (Philips 2773/00 long fine focus). A Göbel mirror (AXO Dresden, C40-0641) is used to convert the divergent polychromatic X-ray beam into a collimated line-shaped beam of Cu Kα radiation ($\lambda = 0.154$ nm). The 2D scattering pattern is recorded by an imaging-plate detector (Fuji BAS1800). Imaging plates were read 5 min after exposure to minimize the effects of rapidly decaying excited states. The 2D image was linearly integrated to obtain $I(q)$ using SAXSQuant software (Anton Paar, Graz, Austria) in the range $0.7 \times 10^{-2} < q < 5$ nm$^{-1}$. Solid samples contained microcrystals with different orientations. Therefore, a rotating cell was used in order to obtain an average signal.

## Results

**Rheology.** Individual micelle solutions at high concentrations showed a solid−liquid transition when the temperature was increased above a critical value $T_c$. It was already reported for E92C18 that $T_c$ increased steeply with increasing concentration until it reached a maximum of 80 °C at about 350 g/L.[8] For $C > 500$ g/L, $T_c$ decreased which is probably related to the lack of sufficient water molecules to fully hydrate all PEO segments. Above 750 g/L, E92C18 could not be completely dissolved in water. In Figure 2a the liquid−solid state diagram of E19C18 is compared with that of E92C18. For E19C18 higher concentrations were needed to form a solid at given temperature. $T_c$ increased steeply with increasing concentration until it reached 80 °C at 350 g/L. E19C18 was insoluble for $C > 400$ g/L so that the expected decrease at high concentrations could not be observed.

When the micelles were mixed, the liquid−solid transition temperature decreased. Figure 2b shows the liquid−solid state diagram for mixtures with $C = 370$ g/L as a function of the weight fraction ($F$) of E19C18. $T_c$ decreased sharply both when small micelles were added to large micelles and vice versa. In the range between $F = 0.35$ and $F = 0.7$ no solid could be produced even at 5 °C. The range of $F$ in which solids could be formed decreased with decreasing PEO concentration.

The storage shear modulus of the solids was almost independent of the frequency and was higher for the smaller micelles. $G'$ decreased with decreasing or increasing $F$ from the extremes (see Figure 3). This effect was not caused by the variation of $T_c$ because we plotted $G'$ at a constant value of $T_c - T = 20$. In any case, the temperature dependence of $G'$ was weak for $T < T_c$.

The viscosity of the pure systems and the mixtures increased with increasing concentration and decreasing temperature. It was shown in ref 8 that the viscosity of pure micelles increases linearly with decreasing temperature down to $T_c$ below which an elastic solid is formed. However, if the temperature quench is rapid, the viscosity can be measured even below $T_c$. In fact, for the mixtures of micelles large hysteresis was found between cooling and heating ramps because the formation of the solid slowed down strongly as $T$ approached $T_c$. The same effect was reported before for mixtures of micelles and linear nonfunctionalized PEO.[8] The viscosity of supercooled samples was either determined directly from fast cooling ramps or extrapolated from data at higher temperatures.

Figure 4 shows the concentration dependence of the viscosity for the pure systems and a mixture at $F = 0.5$. The inset shows

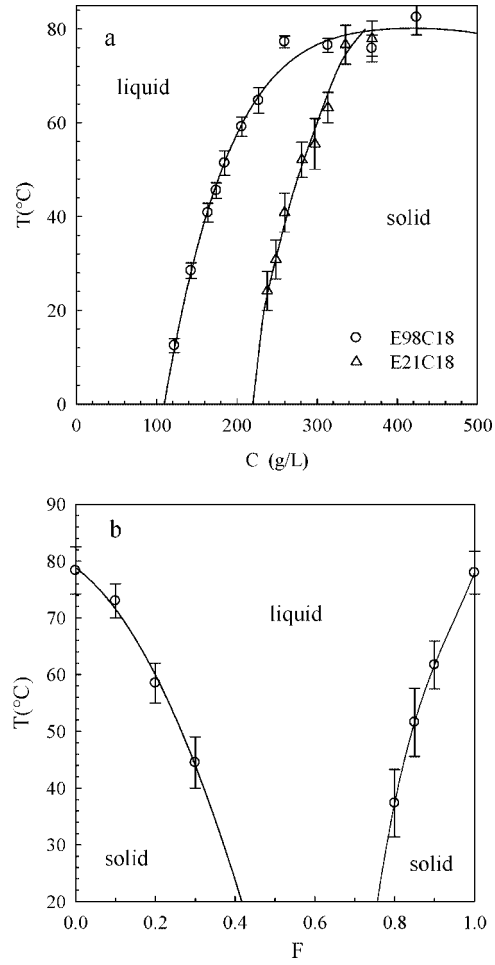


**Figure 2.** Liquid−solid state diagram of pure solutions of small and large micelles as a function of the concentration (a) and for mixtures at $C = 370$ g/L as a function of the fraction of small micelles (b). The lines are guides to the eye.

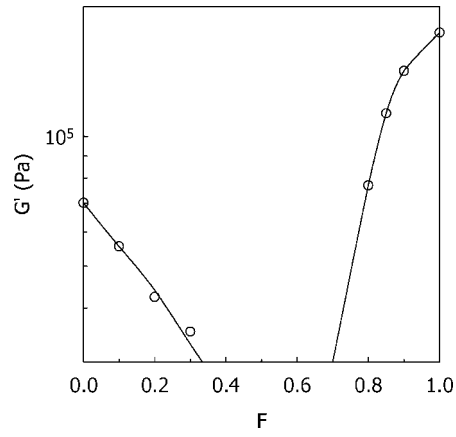


**Figure 3.** Dependence of the storage shear modulus for mixtures at $C = 370$ g/L as a function of the fraction of small micelles at $T_c - T = 20$ °C. The lines are guides to the eye.

the same results plotted as a function of the effective volume ($\phi_e$) of the micelles that can be obtained from light scattering measurements (see below). The increase of the viscosity for the pure systems is similar to that of star polymers with the same number of arms[5] even for supercooled systems indicated by the filled symbols. We stress, however, that stable systems with these higher viscosities cannot be formed with the PEO micelles, while stable suspensions of covalent star polymers or

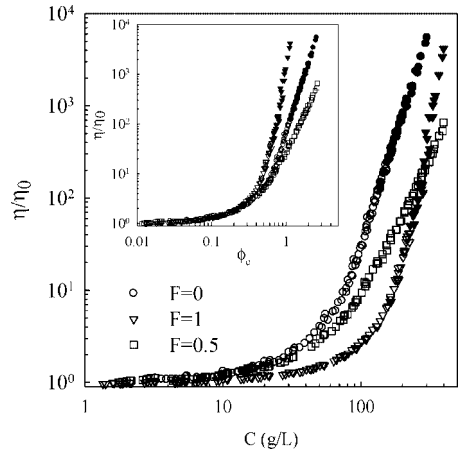


**Figure 4.** Concentration dependence of the relative viscosity for pure solutions of small ($F = 1$) and large ($F = 0$) micelles as well as a mixture at $F = 0.5$. Master curves are shown of data obtained at different temperatures between 5 and 80 °C after horizontal shifts with respect to the reference temperature 20 °C. The filled points represent viscosities of supercooled samples that are solid in equilibrium. The lines are guides to the eye. The inset shows the data as a function of the effective volume fraction.

hard spheres can be made with any viscosity by careful tuning of the concentration.

The sharp viscosity increase occurred at larger $C$ for the smaller micelles because their effective volume fraction at a given $C$ was smaller. Comparison of the results as a function of $\phi_e$ shows that the increase of $\eta$ was steeper for the smaller micelles because the number of arms was higher (see below). The effective volume fraction of the mixed micelles was close to that of the larger micelles. However, the concentration dependence of $\eta$ was weaker than that of either of the pure micelle solutions. Roovers also reported a weaker concentration dependence for so-called fuzzy star polymers with a bidisperse distribution of the arm molar mass in the corona[5] compared to monodisperse star polymers with the same number of arms.

Similar curves were obtained at different temperatures, but the increase occurred at lower $C$ if $T$ was increased. It was shown earlier for E92C18[8] that the data could be superimposed by horizontal shifts, with shift factors that varied linearly with the temperature, and the total shift between 5 and 70 °C was about a factor 1.5. For E19C18 and the mixture master curves could also be obtained by horizontal shifts with similar shift factors. It follows that for all systems increasing the temperature is equivalent to reducing the volume fraction.

Figure 5 shows the viscosity as a function of $F$ for different $C$ at a constant temperature $T = 20$ °C and at different temperatures for a constant PEO concentration $C = 370$ g/L. At low $T$ and high $C$ the viscosity had a clear minimum at intermediate values of $F$. The minimum became less pronounced and shifted to larger $F$ with decreasing $C$ or increasing $T$. At $C = 102$ g/L the viscosity was relatively small and varied almost linearly with $F$ between the values of the pure systems. We note that for hard sphere mixtures similar minima were observed as a function of $F$, but as will be shown below the physical origin is very different.[28]

**Light Scattering.** We investigated the concentration dependence of the osmotic compressibility and the cooperative diffusion coefficient of micelle solutions using static and dynamic light scattering. Figure 6 shows the concentration dependence of $KC/I_r$ for the pure systems and mixtures with $F = 0.5$ at 20 °C. The results at low concentrations show that the weight-average molar mass of the micelles is very close for the two polymers. We are not aware of any particular reason why this should be the case and it could be fortuitous. Using the molar mass of the polymers given above, we find association number $p = 32$ for E92C18 and $p = 105$ for E19C18. $M_w$ was also almost the same for mixtures, not only at $F = 0.5$ as is shown in Figure 6 but for all ratios (data not shown). This observation is consistent both with the formation of a binary mixture of monodisperse micelles and with the formation of a monodisperse solution of mixed micelles.

$KC/I_r$ increased with increasing concentration due to excluded volume interaction. The inset of Figure 6 shows the normalized scattering intensity $I_r/(KCM_w)$, which is proportional to the osmotic compressibility, as a function of the effective volume fraction. $\phi_e$ can be calculated by comparing the initial concentration dependence of $I_r/(KCM_w)$ with the so-called Carnahan−Starling equation for hard spheres[29]

$$\frac{I_r}{KCM_w} = \frac{(1-\phi_e)^4}{1+4\phi_e+4\phi_e^2-4\phi_e^3+\phi_e^4} \quad (4)$$

represented by the solid line in the inset of Figure 6. The effective hard-sphere radii obtained in this way were 7.6 nm for E92C18, 5 nm for E19C18, and 7 nm for the mixture. These values were close to the hydrodynamic radii found in dilute solutions (see below).

Earlier experiments on solutions of E92C18[8] showed that the osmotic compressibility decreased in a way similar to that of star polymers with the same number of arms, except at high concentrations where the decrease became steeper because $p$ increased with increasing concentration. For $C > 150$ g/L a solid was formed, but there was no signature of the liquid−solid transition in the evolution of the osmotic compressibility. The increase of the $KC/I_r$ started at larger $C$ for the smaller micelles because for a given $C$ their volume fraction is smaller. However, as is clearly seen in the inset of Figure 6, the decrease of the osmotic compressibility with increasing $C$ was stronger because the smaller stars contained more arms. For the mixture with $F = 0.5$ the increase was close to that of the larger micelles. In ref 8 we showed that at the highest concentrations the values of $KC/I_r$ are close to those for nonfunctionalized PEO solutions, which means the scattering intensity of the fast mode is mainly caused by concentration fluctuations of strongly overlapping PEO chains.

The effect of temperature was investigated between 10 and 70 °C. The association number was independent of the temperature while the increase of $KC/I_r$ became slightly weaker with increasing temperature. The latter is caused by a decrease of the repulsive interaction between PEO segments in part due to a decrease of the hydration of the PEO segments. As was shown in ref 8, the data at different temperatures could be superimposed by horizontal shifts, i.e., by varying the effective volume fraction of the micelles.

Dynamic light scattering was used to determine the cooperative diffusion coefficient of these systems as explained in the Experimental Section (see Figure 7). The inset of Figure 7 shows $D_c$ normalized by the value extrapolated to zero concentration ($D_0$). $D_c$ increased with increasing concentration because repulsive interaction between the PEO segments dominated the increased friction. Again there was no signature of the liquid−solid transition even though the centers of mass of the micelles were immobilized in the solid. The reason is that the scattered light of the fast mode is due to concentration fluctuations of overlapping PEO segments and does not involve relative motion of the whole micelles with respect to each other. $D_c$ increased more strongly for the smaller micelles, while the increase of the mixed system was close to that of the larger micelles. These results are consistent with the static light scattering results.

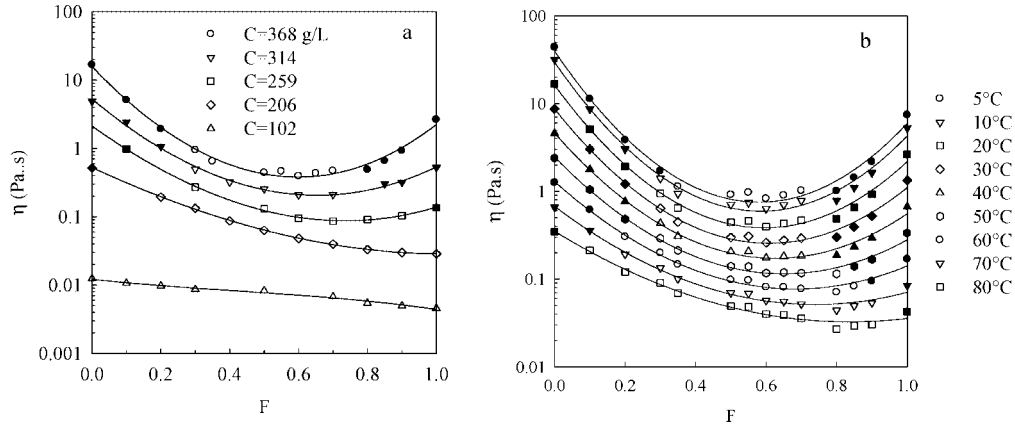


**Figure 5.** Dependence of the viscosity on the fraction of small micelles at 20 °C as a function of the PEO concentration (a) or at $C = 370$ g/L as a function of the temperature (b). The filled points represent viscosities of supercooled samples that are solid in equilibrium. The lines are guides to the eye.

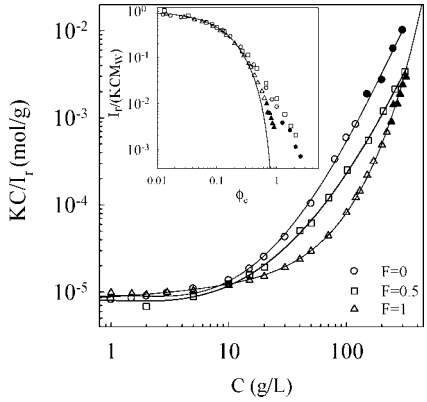


**Figure 6.** Concentration dependence of $KC/I_r$ for pure solutions of small ($F = 1$) and large ($F = 0$) micelles as well a mixtures at $F = 0.5$ at 20 °C. The filled symbols represent systems in the solid state. The lines are guides to the eye. The inset shows the normalized scattering intensity as a function of the effective volume fraction.

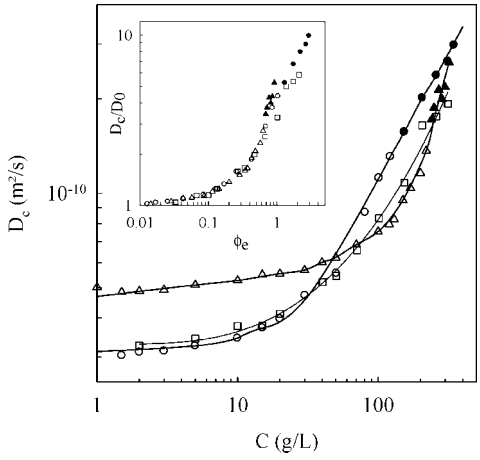


**Figure 7.** Concentration dependence of the cooperative diffusion coefficient for pure solutions of small ($F = 1$) and large ($F = 0$) micelles as well a mixture at $F = 0.5$ at 20 °C. Symbols are as in Figure 6. The lines are guides to the eye. The inset shows the normalized diffusion coefficient as a function of the effective volume fraction.

The $z$-averaged hydrodynamic radius determined from $D_0$ was $R_{hl} = 7.6$ nm for E92C18 and $R_{hs} = 4.8$ nm for E19C18, with no significant temperature dependence. The average hydrodynamic radius of the mixture at $F = 0.5$ was close to that of the larger micelles. This is a strong indication that mixed micelles were formed because for a binary mixture with the same $M_w$,

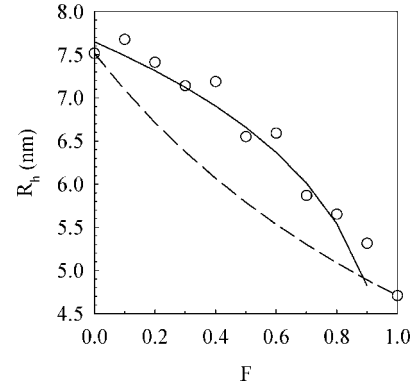


**Figure 8.** Dependence of the hydrodynamic radius of mixtures as a function of $F$. The solid line represents the prediction for monodisperse mixed micelles (eq 6), while the dashed line represents the prediction for binary mixtures of micelles with two different sizes (eq 5).

$R_{hz}$ should be closer to that of the smaller micelle. An unambiguous proof of the formation of mixed micelles was obtained by measuring $R_{hz}$ of dilute mixtures at different $F$. The results are shown in Figure 8 together with the prediction for mixtures of two different micelles and for mixed micelles. The former is simply calculated from the values of the pure systems:

$$R_{hz} = [FR_{hs}^{-1} + (1 - F)R_{hl}^{-1}]^{-1} \quad (5)$$

For the latter we assumed that $R_{hz}$ is determined by the number of long arms in the mixed micelles. Since the molar mass does not significantly depend on $F$, it follows that the fraction of long arms is equal to $(1 - F)$. The model for star polymers proposed by Cotton and Daoud predicts that the radius increases as a weak power law with the number of arms ($R \propto p^{0.2}$) so that

$$R_{hz} = (1 - F)^{0.2}R_{hl} \quad (6)$$

This approach ignores the contribution of the smaller chains that increases with increasing $F$, and eq 6 is clearly incorrect for $F$ close to unity. However, over a broad range of $F$ the experimental results were consistent with eq 6, demonstrating that mixed micelles were formed and not a binary mixture of pure micelles.

**SAXS.** In ref 4 we have shown that E92C18 forms a body-centered-cubic (bcc) phase over a broad range of concentrations and temperatures. The crystal structure forms relatively rapidly if the system is not very close to the critical temperature, although as mentioned above after the solid has formed. Here we show only structures when the steady state was reached.

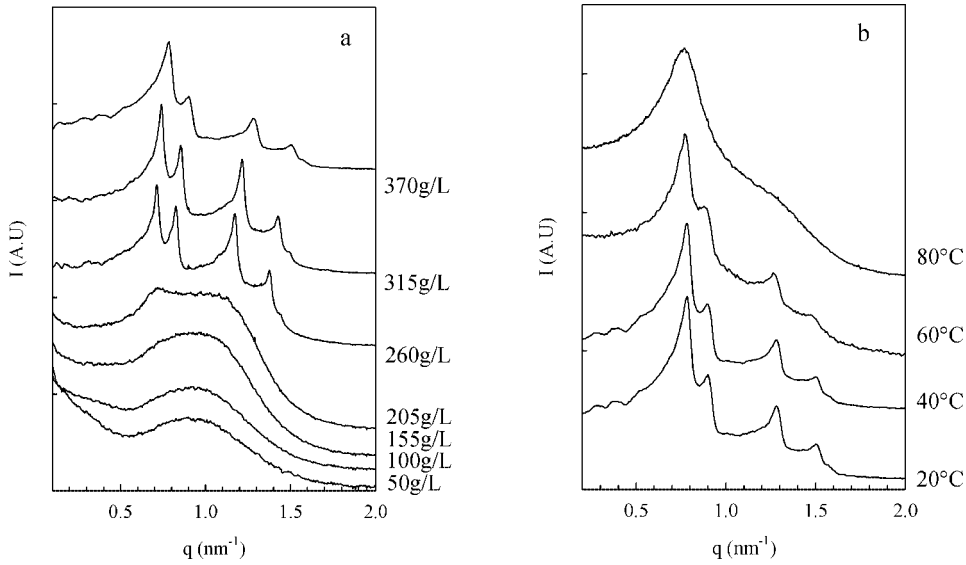


**Figure 9.** Dependence of the scattering intensity as a function of the scattering wave vector for micelles formed by E19C18 at different PEO concentrations at 20 °C (a) or at different temperatures at $C = 370$ g/L (b).

Figure 9 shows that E19C18 formed a face-centered-cubic (fcc) phase in the solid state. Theoretically, a transition from a bcc phase to a fcc phase was predicted for star polymers with increasing number of arms.[13] The transition was observed experimentally for polymeric micelles with decreasing ratio of the corona to core size.[30] The appearance of an fcc phase for the smaller micelles with larger association number is thus not unexpected.

The Bragg peak positions are independent of the temperature and increase weakly with increasing concentration. The distance between nearest neighbors in the crystals can be calculated from the peak positions, giving 9.9 nm for E19C18 and 12.8 nm for E92C18 at $C = 370$ g/L. If we assume that the majority of the material is crystalline, we can calculate the number concentration of micelles and thus their association number. As was discussed in ref 4, the association number of E92C18 increased with increasing concentration from $p = 32$ in dilute solutions to almost 100 at 400 g/L. In the present study we found $p = 83$ at $C = 370$ g/L. The association number of the smaller micelles varied more weakly from $p = 105$ in dilute solutions to $p = 138$ at 370 g/L.

With light scattering we found that the association number was independent of the temperature at low concentrations. The SAXS measurements show that it is also independent of the temperature at high concentrations in the solid state. Notice that the peak position of the liquid order peak at 80 °C is the same as that that of the first Bragg peak. For close packed randomly distributed micelles $2\pi/q_{max}$ represents the average distance between the micelles. This means that the average distance between the micelles in the crystalline state is larger than in the liquid state.

The structure factor of the 50/50 mixtures as a function of the concentration is shown in Figure 10a. With increasing concentration the liquid order became stronger, but no Bragg peaks were observed. The structure factor of the mixture is intermediate between that of E19C18 and E92C18 in the liquid state. At low concentrations the scattering of the core at $q \approx 0.9$ nm$^{-1}$ is more prominent than a simple average of the structure factors of the two polymeric micelles (see Figure 10b), which confirms that mixed micelles were formed.

Figure 11 shows the structure factor as a function of $F$ for a fixed PEO concentration of 370 g/L at 20 °C. For $F \geq 0.8$ an fcc phase was formed, while for $F \leq 0.2$ bcc was formed. In the intermediate range the system had no long-range order. At $F = 0.3$, the liquid state was metastable when it was cooled from high temperatures to 20 °C. At 5 °C the sample formed a bcc phase, which remained when it was heated to 20 °C. Both states at 20 °C are superimposed in Figure 11. Notice that the first peak position is the same in both states.

The planar spacing calculated from the first peak position ($d = 2\pi/q_{max}$) is shown as a function of $F$ in Figure 12. We repeat that $d$ does not depend on the temperature and is the same in the liquid and in the solid state. For close packed randomly distributed micelles $d$ represents the average distance between the micelles. We found that $d$ was significantly smaller than $2R_h$, implying that the micelles are compressed or interpenetrated. $d$ decreased weakly with increasing $F$. This means that the number concentration of micelles increased with increasing $F$ at high concentrations, contrary to dilute solutions where it was almost independent of $F$.

## Discussion

We have shown that mixing PEO with different molar masses end-capped with the same hydrophobic group forms mixed micelles. Joanny et al.[31] developed a theory of micelle formation in mixed diblock copolymer systems in which they neglected the interfacial energy and supposed that the molar mass of both blocks was large. This theory predicts the formation of binary mixtures or mixed micelles depending on the composition. For the present case of identical lyophobic blocks and varying length of the lyophilic blocks, formation of mixed micelles was predicted in agreement with the experimental observations.

Even though polymeric micelles resemble closely star polymers, mixing micelles is different from mixing star polymers.[14,15] In both cases mixing two pure systems in the solid state may lead to melting, but the physical origin is different. Covalent star polymers form binary solutions for which the melting is caused by softening of the repulsive interaction between like-sized stars by depletion of small stars. For large size ratios, it is even possible that the small stars diffuse in the voids left by the jammed large stars. However, polymeric micelles form monodisperse stars with a binary distribution of arm lengths so a different mechanism causes the softening of the repulsion. As mentioned above, softening of the repulsion for covalently bound "fuzzy" star polymers was also observed.

For the system studied here the situation is relatively straightforward when small polymers are progressively incor-

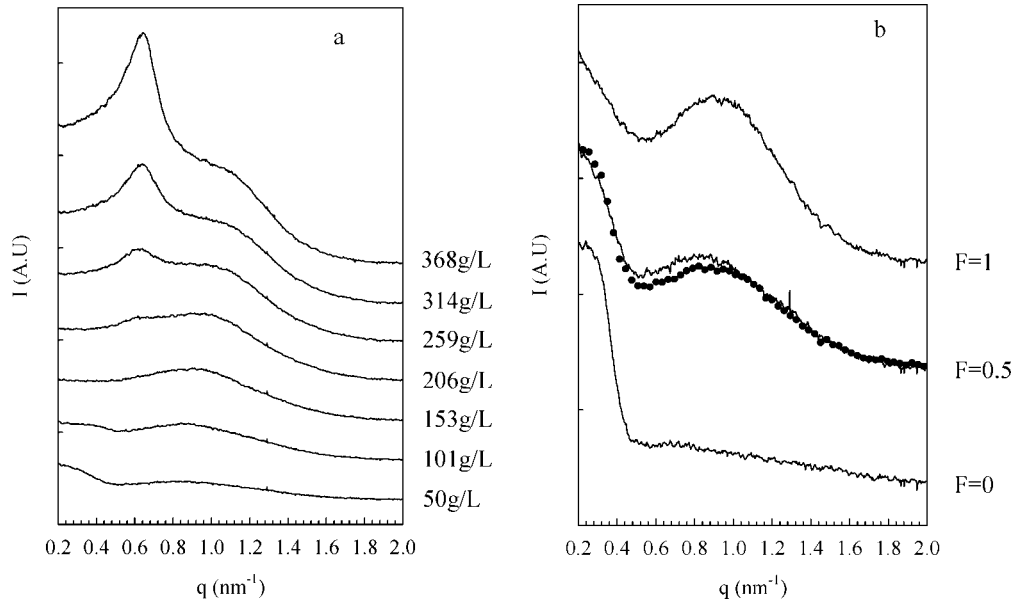


**Figure 10.** (a) Dependence of the scattering intensity as a function of the scattering wave vector for mixed micelles at $F = 0.5$ at different PEO concentrations indicated in the figure at 20 °C. (b) Comparison of the scattering intensity as a function of the scattering wave vector for mixed micelles at $F = 0.5$ with the results for the pure systems at the same PEO concentration (50 g/L). The dotted line shows the average scattering intensity calculated from the pure systems.

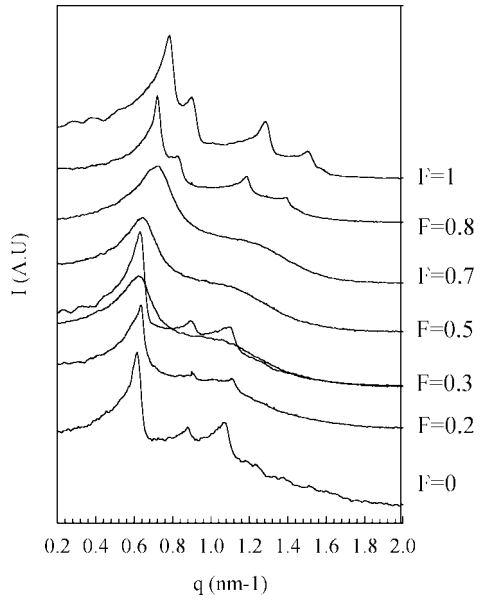


**Figure 11.** Dependence of the scattering intensity as a function of the scattering wave vector for mixed micelles at different $F$ for $C = 370$ g/L at 20 °C. For $F = 0.3$ the structure factors of both the metastable liquid state and the stable crystalline state are shown.

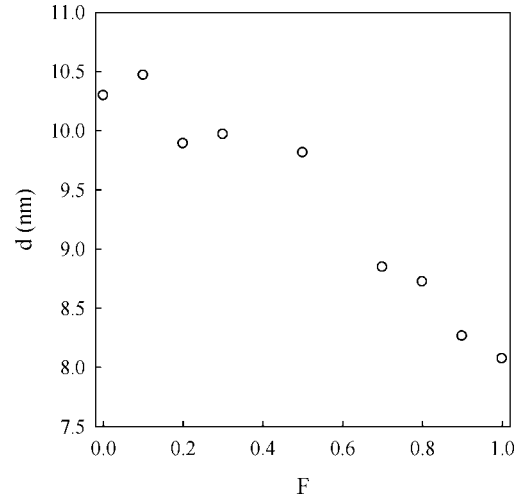


**Figure 12.** Planar spacing ($d = 2\pi/q_{max}$) of mixed micelles as a function of $F$ for $C = 370$ g/L at $T = 20$ °C.

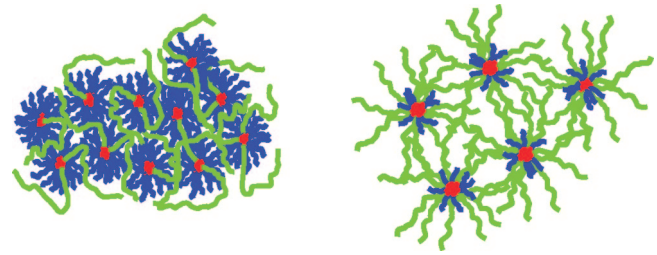

**Figure 13.** Schematic representation of close-packed mixed micelles with an excess of short (left) or long (right) arms.

porated into close-packed large micelles. The small chains contribute much less to the interaction so that the main result is a reduction of the number of long arms per micelle while the number concentration of micelles remains constant. The latter follows because $M_w$ of the micelles does not depend on $F$ at least at low concentrations. Reducing the number of long arms leads to weaker repulsion and at some critical value to melting.

When large polymers are incorporated into small micelles, the situation is quite different (see Figure 13). In this case the number of arms decreases only weakly with decreasing $F$, and the incorporated long arms contribute to the interaction. The situation is similar to that of monodisperse micelles to which nonfunctional chains have been added. Such systems have already been investigated, and it was shown that adding a small fraction of linear chains reduces the repulsion and leads to melting of the solid even if the number of micelles is kept constant.[8,11] The effect increased strongly with increasing length of the linear chains. One may speculate that the linear chains position themselves between the micelles creating in this way defects in the liquid and crystalline order. The same effect can be induced by the part of the long chains that protrudes from the corona.

The hydrodynamic radius of the mixed micelles is determined by the size of the longer arms unless their fraction becomes very small. Therefore, the effect of interaction on the scattering intensity, the diffusion coefficient, and the viscosity starts at approximately at the same concentration as for $F = 0$. However, the interaction is weaker because mixed micelles contain fewer long arms.

SAXS experiments showed a liquidlike order that became more pronounced with increasing concentration or decreasing temperature. Above a critical concentration and below a critical temperature crystalline order could be observed. The appearance of crystalline order coincided with the formation of a solid. Once the solid was formed, the degree of crystalline order stabilized relatively quickly and the system contained domains with crystalline and liquidlike order. The fraction of crystalline material increased with increasing concentration and decreasing temperature and was very small at the liquid−solid transition. The shear modulus of the solid varies very weakly with the temperature while the fraction of crystalline material varies strongly. This indicates that the mechanical response of micelles with crystalline order is not very different form those with liquid order in the solid state. It explains why for deep quenches the shear modulus evolves very little while the crystal phase is formed in the initially fully disorder solid.

The smaller micelles with $p = 103$ formed an fcc phase, while the larger micelles with lower association number with $p = 32$ formed a bcc phase. For star polymers a transition from bcc to fcc was predicted[32] for $p$ larger than about 50. Notice, however, that at high concentrations $p = 83$ for E92C18 yet still a bcc phase was formed.

Yamazaki et al.[16,33] studied mixtures of the same diblock copolymers, but with different smaller PEO chains and alkyl groups (E8C12 and E25C12) for which the liquid−solid transition occurred at higher volume fractions. In the solid state E25C12 formed a bcc phase, while E8C12 formed a hexagonal phase. The lengths of the PEO chains of E25C12 studied by Yamazaki et al. and E19C18 studied here are almost the same. Nevertheless, E25C12 formed a bcc phase and E19C18 an fcc phase. The difference can again be explained by the smaller association number of E25C12 ($p = 26$).[34] Probably for the same reason the solid phase was formed at higher concentrations for E25C12.

Mixing E8C12 and E25C12 also led to melting of the solid and disrupted the crystalline order. The effect of incorporating small chains in large micelles was similar to that shown here, but more large polymers could be incorporated into the solid formed by the smaller polymers than the inverse, contrary to the situation investigated in the present study. The authors attributed this to a larger stability of the hexagonal phase and assumed that mixed micelles where formed. Apparently, when larger chains are protruding out from ordered rodlike micelles the distance between the rods increases, but the order is preserved. Only when the fraction of large chains was high did the hexagonal phase become unstable. It would be interesting to see whether the same is true when large nonfunctionalized chains are added to the hexagonal phase.

## Conclusion

Binary mixtures of hydrophobically end-capped PEO with different molar mass of the PEO and the same alkyl group form mixed micelles in aqueous solutions. If small PEO is present in excess, an fcc phase is formed, whereas in the opposite case, a bcc phase is formed. At high temperatures, the crystalline phase melts and liquidlike order is observed. The temperature above which the crystalline phase melts decreases when small PEO is added to large PEO or vice versa.

A solid−liquid transition occurs at the same temperature as the complete melting of the liquid-crystalline phase. It can be understood in terms of a reduction of the repulsive excluded volume interaction between the micelles as testified by the weaker increase of the viscosity and the osmotic modulus with increasing concentration. When small PEO is incorporated in micelles formed by large PEO, the interaction is reduced because the number of large arms per micelle is reduced. When large PEO is incorporated in micelles formed by small PEO, the interaction is reduced because the large arms stick out of the corona formed by small arms and screened the repulsive interaction. The latter effect is similar to that of adding nonfunctional PEO.

**Acknowledgment.** F.R. acknowledges the Region Pays de la Loire and the Marie Curie Program of the European Union (MRTN-CT-2003-504712) for financial support.

## References and Notes

(1) Hamley, I. W. In *The Physics of Block Copolymers*; Hamley, I. W., Ed.; Oxford University Press: Oxford, 1998; pp 131−220.
(2) Nicolai, T.; Benyahia, L. *Macromolecules* **2005**, *38*, 9794–9802.
(3) Vlassopoulos, D. *J. Polym. Sci., Part B: Polym. Phys.* **2004**, *42*, 2931–2941.
(4) Nicolai, T.; Laflèche, F.; Gibaud, A. *Macromolecules* **2004**, *37*, 8066–8071.
(5) Roovers, J. *Macromolecules* **1994**, *27*, 5359–5364.
(6) Cheng, Z.; Zhu, J.; Chaikin, P. M.; Phan, S.; Russel, P. *Phys. Rev. E* **2002**, *65*, 041405.
(7) Laflèche, F.; Durand, D.; Nicolai, T. *Macromolecules* **2003**, *36*, 1331–1340.
(8) Renou, F.; Benyahia, L.; Nicolai, T. *Macromolecules* **2007**, *40*, 4626.
(9) Stiakakis, E.; Vlassopoulos, D.; Roovers, J. *Langmuir* **2003**, *19*, 6645–6649.
(10) Stiakakis, E.; Petekidis, G.; Vlassopoulos, D.; Likos, C. N.; Iatrou, H.; Hadjichristidis, N.; Roovers, J. *Europhys. Lett.* **2005**, *72*, 664–670.
(11) Yamazaki, R.; Numasawa, N.; Nose, T. *Polymer* **2004**, *45*, 6227–6234.
(12) Yamazaki, R.; Inomata, K.; Nose, T. *Polymer* **2002**, *43*, 3647–3652.
(13) Likos, C. N. *Soft Matter* **2006**, *2*, 478–498.
(14) Zaccarelli, E.; Mayer, C.; Asteriadi, A.; Likos, C. N.; Sciortino, F.; Roovers, J.; Iatrou, H.; Hadjichristidis, N.; Tartaglia, P.; Löwen, H.; Vlassopoulos, D. *Phys. Rev. Lett.* **2005**, *95*, 268301.
(15) Mayer, C.; Stiakakis, E.; Zaccarelli, E.; Likos, C. N.; Sciortino, F.; Löwen, H.; Tartaglia, P.; Vlassopoulos, D. *Rheol. Acta* **2007**, *46*, 611.
(16) Yamazaki, R.; IIzuka, K.; Hiraoka, K.; Nose, T. *Macromol. Chem. Phys.* **2005**, *206*, 439–447.
(17) Sommer, C.; Pedersen, J. S.; Stein, P. C. *J. Phys. Chem. B* **2004**, *108*, 6242–6249.
(18) Higgins, J. S.; Benoit, H. C. *Polymers and Neutron Scattering*; Clarendon Press: Oxford, 1994.
(19) Brown, W. *Light Scattering. Principles and Developments*; Clarendon Press: Oxford, 1996.
(20) Devanand, K.; Seler, J. C. *Macromolecules* **1991**, *24*, 5943–5947.
(21) Venohr, H.; Fraaije, V.; Strunk, H.; Borchard, W. *Eur. Polym. J.* **1998**, *34*, 723–732.
(22) Berne, B.; Percora, R. *Dynamic Light Scattering*; Wiley: New York, 1976.
(23) Brown, W., Ed. *Dynamic Light Scattering. The Method and Some Applications*; Clarendon Press: Oxford, 1993.
(24) Semenov, A. N.; Vlassopoulos, D.; Fytas, G.; Vlachos, G.; Fleischer, G.; Roovers, J. *Langmuir* **1999**, *15*, 358.
(25) Hammouda, B.; Ho, D. L.; Kline, S. *Macromolecules* **2004**, *37*, 6932–6937.
(26) Kinugasa, S.; Nakahara, H.; Fudagawa, N.; Koga, Y. *Macromolecules* **1994**, *27*, 6889–6892.
(27) Duval, M. *Macromolecules* **2000**, *33*, 7862–7867.
(28) Larson, R. G. *The Structure and Rheology of Complex Fluids*; Oxford University Press: Oxford, 1999.
(29) Carnahan, N. F.; Starling, K. E. *J. Chem. Phys.* **1969**, *51*, 635–636.
(30) McConnell, G. A.; Gast, A. P.; Huang, J. S.; Smith, S. D. *Phys. Rev. Lett.* **1993**, *A 71*, 2102.
(31) Sens, P.; Marques, C. M.; Joanny, J.-F. *Macromolecules* **1996**, *29*, 4880.
(32) Watzlawek, M.; Likos, C. N.; Lowen, H. *Phys. Rev. Lett.* **1999**, *82*, 5289–5292.
(33) Iizuka, K.; Hiraoka, K.; Numasawa, N.; Yamazaki, R.; Nose, T. *J. Polym. Sci., Part B* **2005**, *43*, 2474–2483.
(34) Yamazaki, R.; Inomata, K.; Nose, T. *Polymer* **2002**, *43*, 3647–3652.

MA800556U